Exp. Theo. NANOTECHNOLOGY 9 (2025) 449-463 https://doi.org/10.56053/9.S.449

Investigation of nickel-chromium coating effect on corrosion of mild steel pipe by electroplating method

Rana A. Anaee[1,2,], Marwa A. Abbas[1], Saja A. Abdul Maged [1], Shaimaa A. Naser[2], Sinan S. Hamdi[2], Hussain M. Yousif [3], Nabil J. AL-Bahnam[4], Tamara A. Anai[5]*

[1]Department of Materials Engineering, University of Technology, Baghdad, Iraq
[2]Nanotechnology and Advanced Materials Research Centre, University of Technology, Baghdad, Iraq
[3]Ministry of Industry and Minerals, State Company for Steel Industries/Control Tool Room Plant, Taji, Iraq
[4]Department of Physics, College of Science for Women, University of Baghdad, Iraq
[5] Dentistry Basic Science, Tikrit of University, Tikrit, Iraq
[*]) Email: 130033@uotechnology.edu.iq

Received 27/2/2025, *Received in revised form* 19/3/2025, *Accepted* 22/4/2025, *Published* 15/5/2025

Nickel-chromium (Ni-Cr) coating as an alloy is applied on the carbon steel surface by electroplating technology with a thickness of (60-63) µm to investigate the role of this coating through many characterization tests, antibacterial tests, and electrochemical tests. The identification by X-ray diffraction gave peaks at 2θ 45.28° and 52.28°, related to deposit α– (Cr, Ni), confirming the deposition of Ni-Cr alloy as a coating. Scanning electron microscopy gave a dense compact layer over the coated sample, and atomic force microscopy showed more ordering in particles with higher roughness (increasing from 2.26 to 2.73 nm). The observation of antibacterial examination indicated the complete inhibition zone for the coating layer. The electrochemical observations gave the more noble potentials and less current densities for the coated sample compared with the uncoated one at a constant temperature, with good protection efficiencies ranging from 99.82 to 99.95%. The change in free energy is less spontaneous for corrosion in the coated sample (where it changed from -149.093 to -17.8332 kJ.mol^{-1} for uncoated and coated, respectively, at 30°C), in addition to getting less entropy (shifting from 0.46011 to 0.34228 kJ.mol^{-1}.K^{-1} after coating) and obtaining less exothermic behavior after coating, changing from -212.30 to -165.84 kJ.mol^{-1} at 30°C.

Keywords: Carbon steel; Coating; Potentiostatic; Ni-Cr layer.

1. INTRODUCTION

Some factors in soil can increase the rate of external corrosion on the pipelines such as the moisture that increase the movement of ions through the soil and increase the electrical conductivity and then the corrosivity, also the high contents of salts due to poor drainage, the higher contents of oxygen, soil composition and differences in aeration. The type of soil can affect the rate of damage of the coating including heavy clay soils, rocky soils and moisture content. Therefore, there are many attentions are appeared to development of coatings to have better performance, longer life and withstand high temperatures and soil movement, and also be eco-friendly. In general, the soil has low corrosivity due to low conductivity, but it has disadvantage in applying cathodic protection to pipes due to lowing in flow current and this can increase corrosion to a greater extent. The metallic coatings can achieve the resistance to corrosion by three mechanisms: The first is form a passive film as compact and dense oxide act as barrier for blocking anodic sites such as Cr- based or Al- based coatings, the second behave as a sacrificial anode such as Zn which has a potential of (-0.76 V) that regard more active than many metals and alloys and work as an anode to protect the structure (cathode), and the third act a soluble ion behave as corrosion inhibitors such as Ce^{3+} ions [1-3].

Many techniques of coating can be used to protect pipes; some of these coatings are difficult to be applied and cannot bond to the pipes surface in addition to presence holes, voids, other defects. The coatings that attached to soil may be degraded due to moisture. Therefore, long – time coatings begin to use such as epoxy products as cold applied types, wax materials and grease products. On the other hand, wet epoxies and dry powder slowly degrade over time and have good dielectric properties but they do not have mechanical strength. The metallic coatings enhance the corrosion resistance of many metals in different environments within wide range of temperatures and do not subject to thermal degradation compared with organic coatings. Metallic diffusion coatings can enhance the resistance of carbon steel especially Ni- or Cr- based coating. Ni-Cr alloys as coating are widely used because of their properties such as high hardness, abrasion resistance, corrosion resistance, high strength and elastic modulus due to formation of the (Cr_2O_3) protective film on the metallic surface. Therefore, many researches took attention to apply Ni-Cr coatings by different techniques especially electrodeposition [4-9]. There are many researches related to the protection a pipe in soil and mud using coating techniques with different materials such as study the effect of ions concentration that presented in the moisture within four types of soil on corrosion of steel by Ishaq et al. in 2015 [10] followed by investigation the role of nano Al_2O_3 doped polypyrrole coating to protect steel in two simulated soil media by Rana et al. in 2017 (11), and then study the effect of HCO_3^- and Cl^- ions on pitting of steel in simulated soil medium by Mingyang et al. in 2022 (12). On the other hand, various materials are added with nickel to apply coating included (ZnO), ($P-ZnO$), ($P-SiC$) and ($P-Al_2O_3$) [13-17].

Due to importance of maintaining the pipelines and increases their life time to more extent, the innovation and significance methods must achieve to external wall of the pipes by selection the available technique and more resistant materials to apply the coating. The aim of present research is related to study the role of Ni-Cr coating to protect steel against corrosion in simulated soil medium at four temperatures in addition to characterization the coating layer by XRD, SEM and AFM as well as testing the antibacterial behavior.

2. METHODOLOGY

2.1 Materials and coating process

Steel (St 37) according to (DIN) with chemical composition (wt%) of (0.165 C, 0.443 Mn, 0.087 Si, 0.007 P, 0.019 S, 0.004 Cr, 0.002 Mo, 0.011 Cu, 0.027 Ni, 0.0008 V, 0.039 W, 0.011 Al and Bal. Fe) [18] is used as substrate to apply a coating layer on it. Plating method included a combination of the

metallic elements to achieve good properties of adhesion and resistance. Ni-Cr layer is deposited by electroplating method to get thickness of (60-63μm).

Nickel-Chromium electroplating is done by electrolytic deposition after cleaning and getting free-dirt surface for steel substrate. This technology needs a source for metallic ions (Ni^{2+} & Cr^{3+}) as sulfate salts (electrolytic bath, [19], the substrate as cathode and nickel rod as anode as well as some additions to increase the electrical conductivity and mask to obtain regular coating layer with conditions as listed in Table 1, the experimental setup of procedure is shown in Figure 1- (a) and (b).

Table 1 Composition and conditions of electrolytic bath.

Parameter	**Details**
Materials coating (Ni-Cr)	50 g/L $NiCl_2$, 300 g/L$NiSO_4$ 50 g/L $CrCl_3$, 300 g/L $Cr_2(SO_4)$ 30 g/L H_3BO_4
Current	$\sim 6A$
Potential	$\sim 20\ V$
Time	$45\ min$
Temperature	40^oC
Stirring	$200\ rpm$

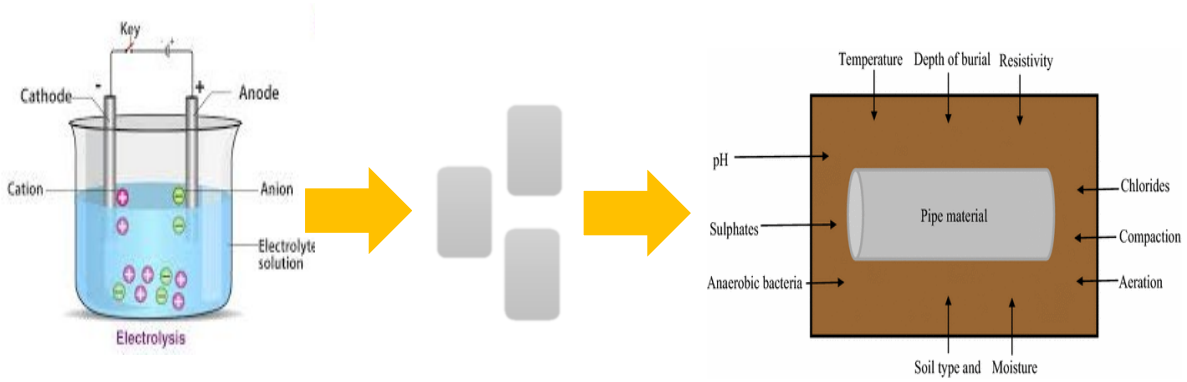

(a)

(b)

Figure 1 Experimental setup to protect pipe in soil by coating (a) and corrosion test (b).

b. Characterization techniques

Many techniques are used to identify the coated samples involved X-ray diffraction (XRD) from *Shimadzu*. Scanning electron microscopy (SEM) from *TESCAN* also used to characterize the morphology of coating layer on carbon steel, while atomic force microscopy (AFM) is used to show the topography of coating layer in addition to calculate surface roughness and average diameter for uncoated and coated samples that affected formation galvanic cells on the surface.

c. Electrochemical properties measurement

Potentiostat from *CorrTest* is used to test the electrochemical behavior for uncoated and coated samples through record the potential as function to time after (60 sec.) of immersion, and then Tafel plots are recorded to estimate the corrosion data including the potentials and current of corrosion (i.e., E_{corr} and i_{corr}) and Tafel slopes (b_c and b_a) using simulated soil medium as corrosive environment including (0.01M NaCl+0.01M $NaHCO_3$) [20]. Other related corrosion data can be calculated to discuss the role

of current coating including polarization resistance (R_p) and protection efficiency ($PE\%$) using the following formula [21, 22]:

$$R_p = \frac{b_c \times b_a}{2.303\, i_{corr}(b_c + b_a)} \quad (1)$$

$$PE\% = \left[1 - \frac{i_{corr\ coated}}{i_{corr\ uncoated}}\right] \times 100 \quad (2)$$

The porosity percentage ($PP\%$) also calculated using polarization resistance for uncoated ($R_{p,uncoated}$) and coated ($R_{p,coated}$) surface with the corrosion potential difference (ΔE_{corr}) between uncoated and coated case as follow [23, 24, 25]:

$$PP\% = \frac{R_{p,uncoated}}{R_{p,coated}} \times 10^{-\Delta E_{corr}/b_a} \times 100 \quad (3)$$

3. RESULTS AND DISCUSSION

3.1 Characterization of Ni-Cr coated carbon steel

X-ray diffraction for coated sample is investigated to record the peaks as shown in Figure 2, at 2θ 45.28° and 52.28°, these peaks are similar to that appear for Ni card according to (JCPDS) of 03-1043, with did not appear the peaks for pure chromium [26] confirming the incorporation between Ni and Cr and closed to α– (Cr, Ni) card according to (JCPDS) of 26-0429. The nickel metal has good role behave as binder in coating as observed by Lin et al. [27] who deposited the rare metal (Gd) in presence of (Ni) in addition to its role in Dopamine self-polymerization, where the Dopamine membrane polymerized on the top of metallic coatings of (Cu-Ni-Gd) acting as a barrier for corrosion environments. These two metals (Ni & Cr) add advantage to base materials related to excellent corrosion resistance by Ni and easy to passivation by Cr.

Two images by scanning electron microscopy are taken for uncoated and coated samples at two magnifications as shown in Figures 3 and 4. The images of uncoated carbon steel indicated the scratches obtained by grinding and polishing with flat surface and little roughness to get adhesion for coating. The SEM images for coated sample show full coverage and compact dense layer of coating with microcracks due to chromium content as observed by Hossein et al. when deposited Ni-Cr coating by pulse – electrodeposition [28]. This produced compact dense layer will enhance the protectiveness of surface against corrosion.

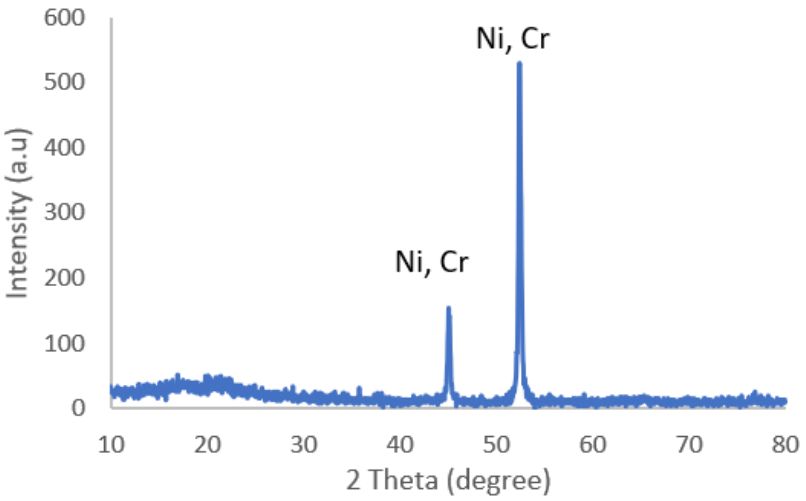

Figure 2 XRD analysis for coated carbon steel sample.

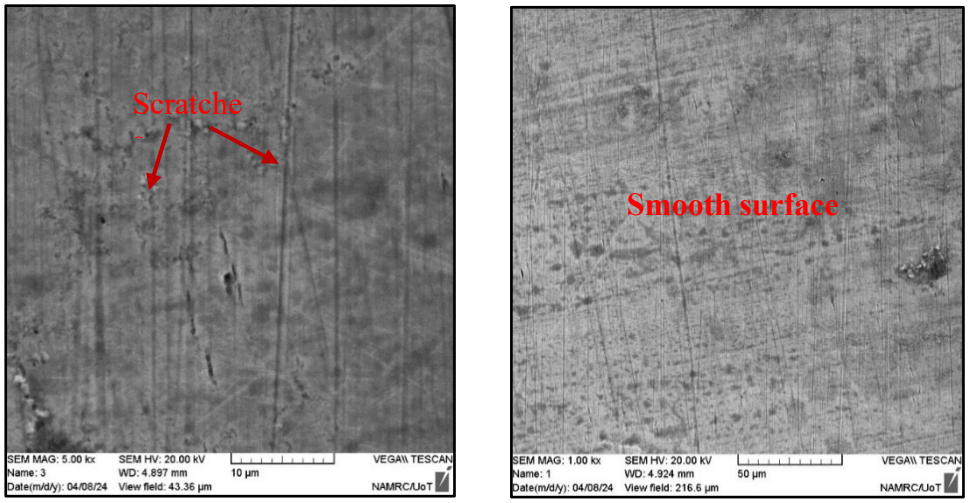

(a) Uncoated sample

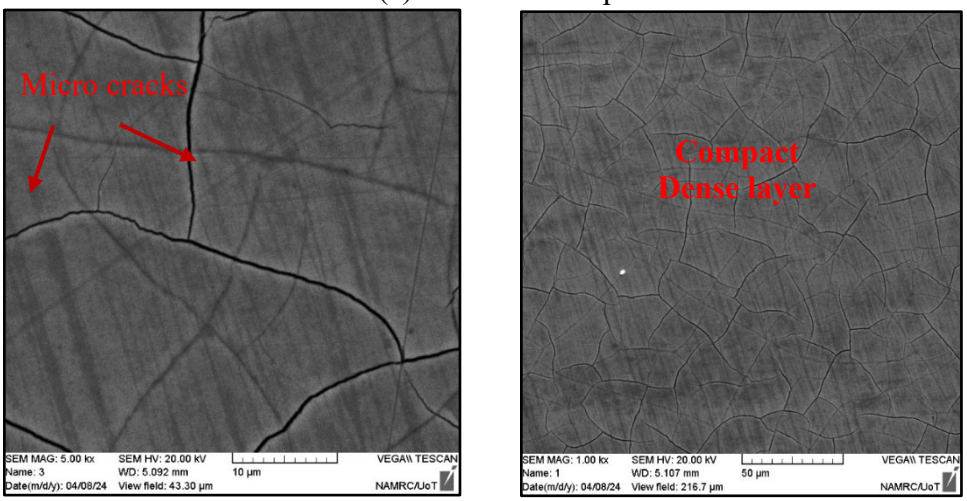

(ii) coated sample

Figure 3 SEM images for uncoated (i) and coated (ii) carbon steel samples at two magnifications (a) 10 µm and (b) 50 µm.

The characterization by atomic force microscopy represents the topographical analysis for surface to support the morphological analysis by scanning electron microscopy, as seen from Figure 3 the valleys and peaks on the surface are decreased with less deeps for coated sample due to coating layer of Ni-Cr alloy in spite of the presence of micro cracks. The average surface roughness is increased from 2.26 nm for uncoated sample to 2.73 nm for coated once due to precipitation of a brittle phase for lath-shaped Ni_3Cr_3 [28], and also observed by Hiyam et al. when they apply $Nb_2O_5 - Ni$ coating on carbon steel [29, 30, 31]. Figure 5 indicates the accumulation distribution of particles with their diameters on the surface, it can be seen that the diameters after coating is very increased confirming the deposition of coating layer, where the percentage of ≤10% is 14 nm and 200 nm for uncoated and coated surface respectively, while the percentage of ≤50% is 34 nm and 500 nm for uncoated and coated surface respectively, and finally the percentage of ≤90% is 56 nm and 750 nm for uncoated and coated surface respectively to get average diameter for uncoated surface equal to 35.10 nm and for coated once is 511.88 nm (because of lath-shaped Ni_3Cr_3 phase). This is attributed to incorporation between coating elements (Ni & Cr) rather than deposition as separated particles.

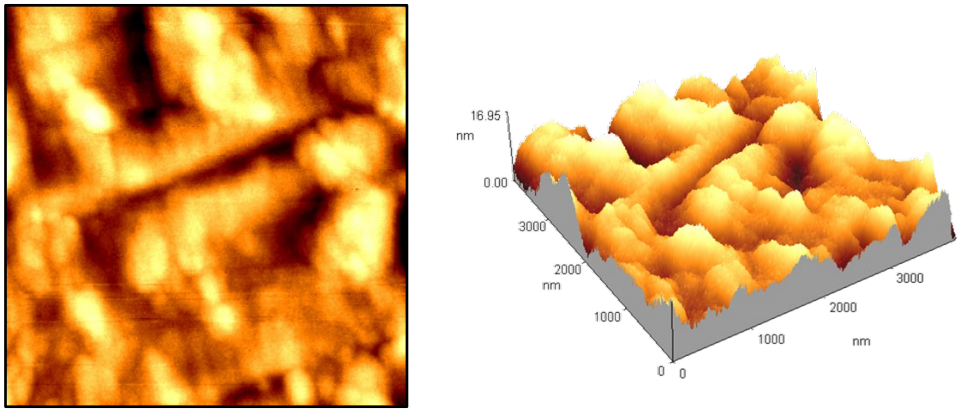

(i) Uncoated carbon steel sample

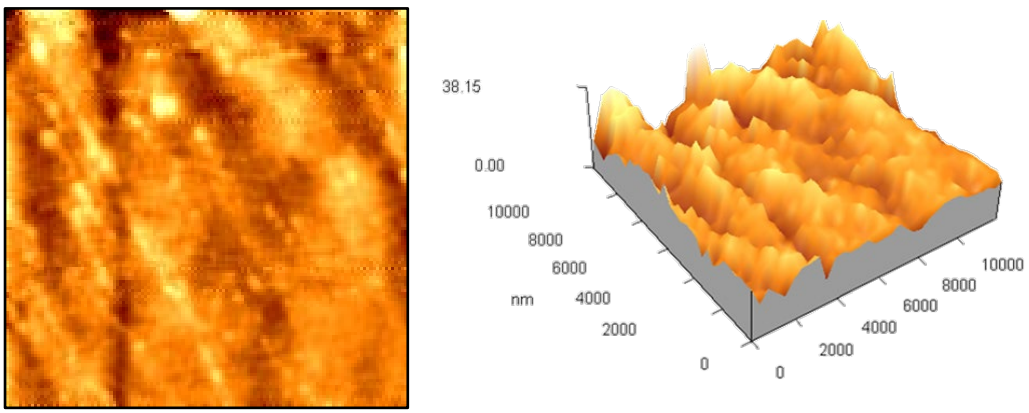

(ii) Coated carbon steel sample

Figure 4 AFM images (2D & 3D) for uncoated (i) and coated (ii) sample.

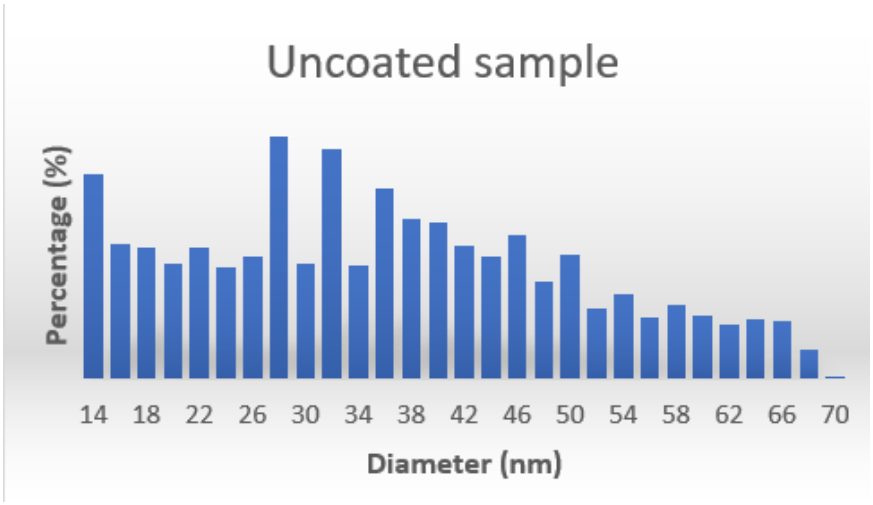

(i) Uncoated carbon steel sample

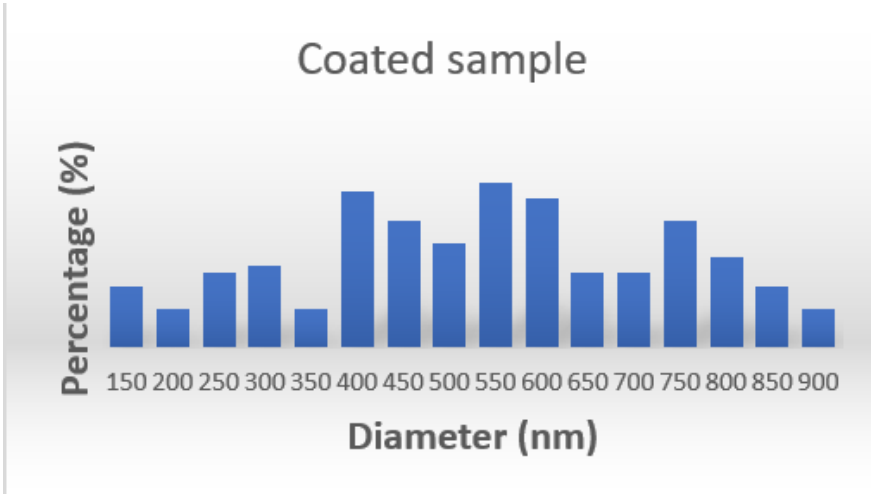

(iii) Coated carbon steel sample

Figure 5 Granularity accumulation distribution for uncoated (i) and coated (ii) samples.

3.2 Identification of antibacterial behavior of Ni-Cr coated surface

Any coating can attract by microorganisms especially in soil and mud because of presence all living conditions for them, therefore, the selected coating for pipelines that buried in mud must be protected against biological corrosion (MIC). In soil, there are many types of bacteria Azotobacter, Agrobacterium, Azospirillum, Gluconobacter, Herbaspirillum and Flavobacterium that represented the examples for free living and nitrogen fixing bacteria, but E. coli usually uses by biologists due to its relative simplicity and the easing of propagation in the laboratory studies, also it consists of ≈ 4.6 million base pairs and encodes about 4000 different proteins. Figure 6 shows completely inhibition zone for coated sample, where the corrosion occurs in all side except the coated once without any growth of bacteria. On the other hand, some bioactivity roles are observed by Shaimaa et al. when they investigated the in vivo study for Ni-Ti coating [32], Gd-Ni-Ti coating [33] and Sm-Ni-Ti coating [34]. This means that nickel metal has an important role to prevent bacteria to be formed.

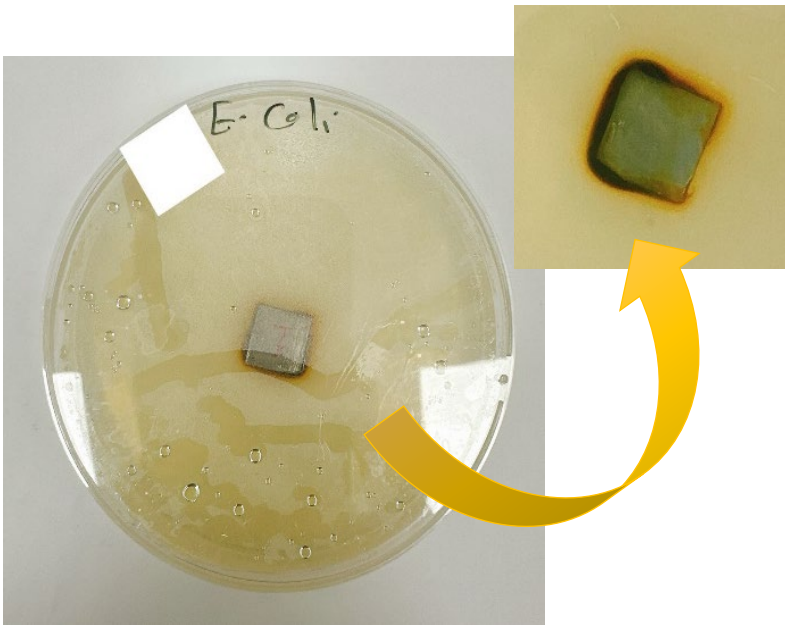

Figure 6 Antibacterial test for coated sample.

3.3 Corrosion behavior of carbon steel

It is known that the most common type of corrosion is take place by electrochemical mechanism, i.e., through formation of anodic and cathodic sites on the metallic surface. Application of coating try to reduce or minimize the reactions that occur at these sites, either by controlling one of reactions (One site) or both reactions (Anodic and cathodic sites). The first step to predict corrosion behavior began by recording the potential respected to time (Experimental time) to show steady state and recording the stability at Material/Electrolyte interface and know the open circuit potential (E_{oc}). Figure 7 show Potential – time behavior at 30^oC for uncoated and coated carbon steel samples with record all potentials at four temperatures (30^oC, 40^oC, 50^oC and 60^oC) that take the sequence of -0.687, -0.778, -0.798 and -0.800V for uncoated and -0.044, -0.089, -0.093 and -0.082 V for coated sample respectively. The results indicate the large shifting of (E_{oc}) in noble direction after coating by Ni-Cr alloy, i.e., giving more stability for metallic surface with corrosive medium [26].

The polarization curves (Figure 8, a-d) are the good tool to the prediction of behavior for samples in corrosive medium (Simulated soil medium) through recording the cathodic and anodic behavior of surface and know the electrochemical data. The hump shape in anodic section for uncoated sample refer to occurring the concentration polarization ($O_2 + 4e + 4H^+ \rightarrow 2H_2O$) with activation polarization ($2H^+ + 2e \rightarrow H_2$) through the reduction of oxygen at cathodic sites. While with coating, this second reduction reaction is disappeared.

At anodic section, the curve is shifted toward less current density with tendency to produce passive film on the surface and then reduce the dissolution of metals ($M \rightarrow M^{n+} + ne$) from base alloy. This reduction in reactions that occur at cathodic and anodic sites after coating can be identified by cathodic and anodic Tafel slopes (b_c&b_a) in Table (2) which reduced after coating at constant temperature. Also, the role of Ni-Cr coating to enhancing the performance of substrate can be shown through the shifting of corrosion potentials (E_{corr}) toward noble direction and large reduction in corrosion current densities (i_{corr}) after coating. The shifting to more positive potential confirms the producing of nickel oxide and chromium oxide as passive layers as illustrated in the characterization tests [35,36].

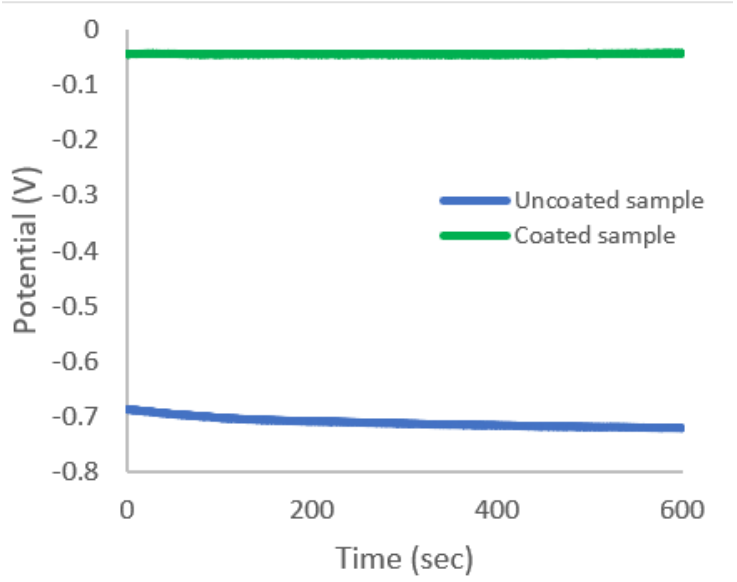

Figure 7 Potential – time behavior at 30^oC.

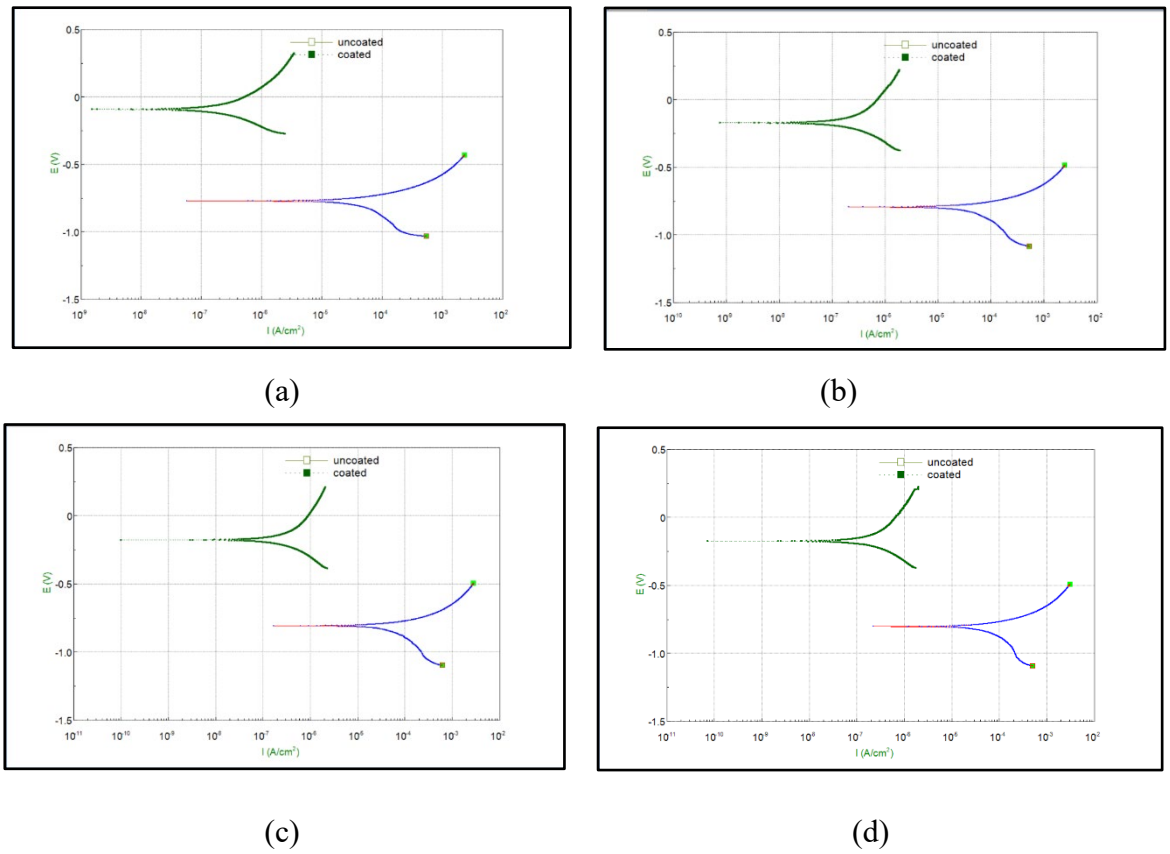

(a) (b)

(c) (d)

Figure 8 Polarization (Tafel) plots for samples at four temperatures; (a) 30^oC, (b) 40^oC, (c) 50^oC and (d) 60^oC.

Table 2 Measured data of corrosion in simulated soil medium at four temperatures.

Sample	$Temp.$ $(°C)$	$-E_{corr}$ (V)	i_{corr} $\times 10^{-5}$ $(A.cm^{-2})$	$-b_c$ $(mV$ $/decade)$	$+b_a$ $(mV$ $/decade)$
Uncoated	30	0.7725	6.156	423.28	134.09
	40	0.8156	2.249	124.4	55.267
	50	0.8392	4.840	261.45	86.431
	60	0.8441	7.149	374.32	109.21
Coated	30	0.0924	0.00452	22.589	40.319
	40	0.1261	0.00391	33.713	35.634
	50	0.1352	0.00407	30.698	30.065
	60	0.1485	0.00322	30.901	32.91

The results of resistance indicate the large increasing for coated surface with giving excellent efficiencies at all experimental temperatures Table (3). The nickel (Ni) shares by forming passive layer and repairing the destroyed layer of passive film for base steel pipeline, also chromium (Cr) has a perfect passive film as (Cr_2O_3) that confirm the immunity of surface to dissolution in corrosive medium and then the treatment of carbon steel's surface will like stainless steel by its nobility. The good compact layer of coating that give enhancing to passivity can see it by low porosity percentages that calculate by eq. (3) and listed in Table (3).

The cathodic Tafel slope (b_c) for uncoated sample which is greater than expected value of ($\frac{2.3\times 2R\times T}{F}$), i.e., $b_c = 120\, mV.dec^{-1}$ or $\alpha = 0.5$ for the Volmer-Tafel mechanism [34]. This value is related to reaction of the hydrogen evolution which is represented as important reaction because it is a common cathodic reaction for corrosion of metals and alloys in all corrosive media, and also this reaction is generate hydrogen atoms that can pass into the lattice structure and lead to occurring the embitterment. The values of Tafel slopes that greater than ($120\, mV.dec^{-1}$) are usually refer to anomalous behavior and it cannot be predicted for any mechanism [37].

On the other hand, the cathodic Tafel slopes (b_c) that are less than ($-120\, mV.dec^{-1}$) suggest the chemical desorption step through the diffusion of adsorbed H atom into metal surface, either pushing H_2O molecules aside until to form H_2 molecule and then escapes to medium or by threading (H atoms) their way after adsorbing on H_2O molecules. This chemical step is not involving charge transfer and the rate determining step ($r.d.s$) will be proportional to the concentration or coverage (θ_H) of adsorbed hydrogen (H_{ads}) followed by the discharge reaction, this process is called chemical desorption and has expected value of (b_c) equal to ($-30\, mV.dec^{-1}$) as shown for coated surface. While, occurring the electrochemical desorption step refer to more complex process due to summing among the reaction of adsorbed hydrogen (H_{ads}), protons (H_3O^+) and electrons (e) on the metal surface, this leads to high coverage (θ_H) and the expected value of (b_c) is ($-50\, mV.dec^{-1}$). The main reactions can discuss this above explanation are:

$$H_3O^+_{(Bulk\ solution)} \xrightarrow{Diffusion} H_3O^+_{(Metal/solution\ interface)} \quad (4)$$

Followed by the discharge reaction as follow:

$$H_3O^+ + M + e \rightarrow M - H + H_2O \quad (5)$$

The reaction of a chemical desorption occurs as follow:

$$M - H + M - H \rightarrow 2M + H_2 \quad (6)$$

In some cases, the above two steps may occur together to form one electrochemical desorption as:

$$M - H + H_3O^+ + M_{(Electrode)} \rightarrow 2M + H_2 + H_2O \quad (7)$$

The two mechanisms (reduction & dissolution) are suggested to formation of passive film on the metallic surface, i.e., the $precipitation-oxidation$ mechanism and $solid - state$ mechanism [38]

Table 3 Measured data of corrosion inhibition in simulated soil medium at four temperatures.

Sample	$Temp.$ $(°C)$	$R_p \times 10^2$ $(\Omega.cm^2)$	$PE\%$	$PP\%$
Uncoated	30	7.182	---	---
	40	7.388	---	---
	50	5.827	---	---
	60	5.135	---	---
Coated	30	1390.81	99.92	0.5103
	40	1923.81	99.82	0.3731
	50	1620.48	99.91	0.3529
	60	2149.09	99.95	0.2354

The change in free energy (ΔG) represent an important thermodynamics parameter, which is directly related to the work capacity (or maximum electric energy) for corrosion system and it, is accompanied to an electrochemical reaction as follow:

$$\Delta G = -nFE_{corr} \quad (8)$$

Where $n$the number of electrons is involved in the electrochemical reaction and F is the Faraday constant (96500 C.mol^{-1}).

It is clear from the data that the corrosion of uncoated sample is more spontaneous process than the coated other. Also, the change in the entropy (ΔS) is related to thermodynamic of the corrosion process and can be estimated from the slope of the relation that presented in Figure 9 according to the following formula [39, 40]:

$$\Delta S = -\frac{\Delta G}{dT} \quad (9)$$

It is known that (ΔS) is reflect the change in the order and orientation of the species that form the hydrated (or solvated) metal ions in the corrosive medium, the values of (ΔS) are positive (as listed in Table 4) and the coated case has less positive value than uncoated once suggesting the decreasing in disorder for solvated states (S_2) compared with the atomic state (S_1) of metal structure, where in corrosion of

uncoated sample the surface is completely covered by ferrous ions at electrical double layer. While in corrosion of coated sample the anodic sites are decreased and the number of iron (II) ions is less and then the solvated ions also less (3).

Finally, the enthalpy changes (ΔH) that associated the corrosion process can be calculated according to the following formula [41, 42]:

$$\Delta H = \Delta G - T\Delta S \quad (10)$$

This parameter reflects the nature of reaction as exothermic or endothermic, and the results in Table (2) show the exothermic process, but it is decreased for coated case due to decreasing in reactions on the metallic surface [43].

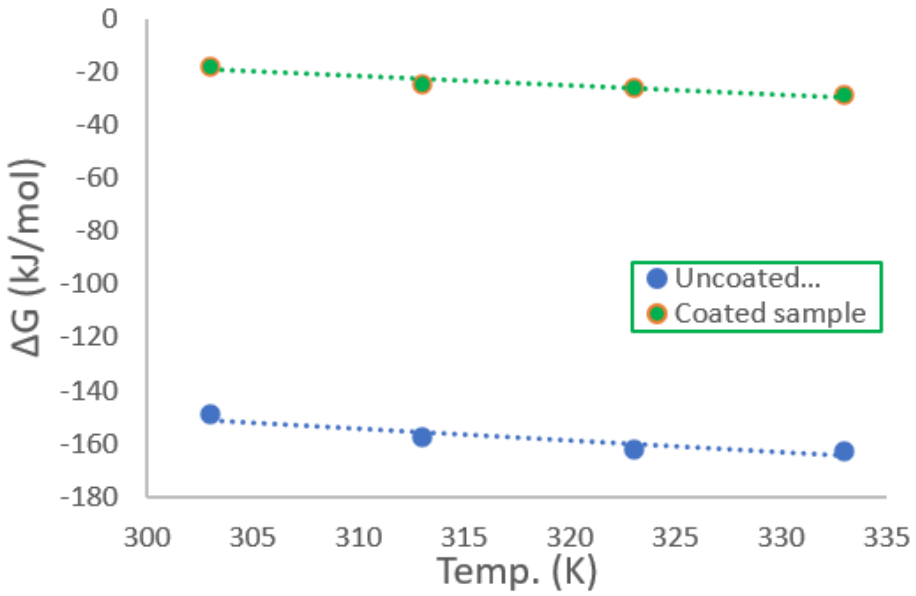

Figure 9 Variation of (ΔG) with temperature (T).

Table 4 Measured data of thermodynamic function for corrosion in simulated soil medium at four temperatures.

Sample	$Temp.$ $(°C)$	ΔG $(kJ.mol^{-1})$	ΔS $(kJ.mol^{-1}.K^{-1})$	ΔH $(kJ.mol^{-1})$
Uncoated	30	-149.093	0.46011	-212.30
	40	-157.411		-218.85
	50	-161.966		-223.56
	60	-162.911		-224.64
Coated	30	-17.8332	0.34238	-165.84
	40	-24.3373		-186.09
	50	-26.0936		-192.11
	60	-28.6605		-196.40

4. CONCLUSIONS

Application of Ni-Cr coating by electroplating technique gave very good protection for carbon steel surface as pipes that contact with soil and mud through testing the corrosion behavior of uncoated and coated samples in simulated soil medium at four different temperatures. The obtained efficiencies were ranged between 99.82 to 99.95 % in addition to shifting the corrosion potentials to the nobel direction confirming the role of coating as passivation (anodic protection) with low porosity percentages that deceased with increasing temperature for applied coating at different temperatures. The applied coating was characterized by different method including XRD, SEM and AFM by indicating the presence of nickel, chromium and Ni_3Cr_3 phase that were assist to produce metal oxides and giving compact dense layer that able to protect pipes for longer time. The tested antibacterial role gave good result due to appear inhibition zone in spite of increasing surface roughness from (2.26 nm) to (2.73 nm) after coating. Many data were calculated from corrosion data and all of them confirmed the protection role of Ni-Cr coating for carbon steel in experimental conditions through decreasing the spontaneous of corrosion with decreasing the disorder of corrosion product after coating.

Funding

All authors have not disclosed any funding.

Author Contributions

Rana A. Anaee, Marwa A. Abbas and Nabil J. AL-Bahnam: Achieving the experimental procdure.
Saja A. Abdul Mageed and Hussain M. Yousif: Applying coating.
Shaimaa A. Naser and Sinan S. Hamdi: Analysis the XRD and SEM data.
Mays A. Anaee and Tamara A. Anai: Analysis the corrosion and AFM

Competing interest

All authors declare that they have no competing interests.

References

[1] N. Najm, A. Ataiwi, R. Anaee, Mater. Today 62 (2022) 4551
[2] R. Shawqi, N. AL-Bahnam, M. Anaee, AIP Conf. Proc. 2414 (2023) 030008
[3] A. Al-Ghaban, H. Abdullah, R. Anaee, A. Khadom, J. Electrochem. Sci. Eng. 13 (2023) 115
[4] Y. Xuetao, W. Yu, Surf. Coat. Technol. 202 (2008) 1895
[5] X. Li-jian, G. Zhu-qing, T. Jian-xin, H. Quan-guo, H. Nong-yue, D. Jing-jing, J. Cent. South Univ. Technol. 14 (2007) 181
[6] A. Sheibani, S.R. Allahkaram, S. Mahdavi, Surf. Coat. Technol. 281 (2015) 144
[7] M.R. Etminanfar, M. Heydarzadeh Sohi, Thin Solid Films 520 (2012) 5322
[8] C. Huang, C.K. Lin, C.Y. Chen, Surf. Coat. Technol. 203 (2009) 3686
[9] Badis Bendjemil, Maram Mechi, Khaoula Safi, Mounir Ferhi, Karima Horchani Naifer, Exp. Theo. NANOTECHNOLOGY 8 (2024) 51
[10] T.I. Gezawa, G. Gangha, N.P. Rajamane, R. Ganapathy, Int. J. Res. Eng. Technol. 4 (2015) 402
[11] R. Anaee, H. Abdullah, Gh. Alsandooq, Eng. Technol. J. 35 (2017) 943
[12] M. Gao, H. Wang, Y. Song, E.H. Hou, J. Mater. Res. Technol. 21 (2022) 3014.
[13] S. Uppada, R. Koona, V. Chintada, Aust. J. Mech. Eng. 22 (2024) 603
[14] V.B. Chintada, R. Koona, Mater. Res. Innov. 24 (2020) 67
[15] S. Uppada, R. Koona, V.B. Chintada, R. Koutavarapu, Silicon 15 (2023) 793

Exp. Theo. NANOTECHNOLOGY 9 (2025) 449-463
[16] V.B. Chintada, R. Koona, T.R. Gurugubelli, Adv. Mater. Process. Technol. 8 (2022) 945
[17] V.B. Chintada, T.R. Gurugubelli, R. Koutavarapu, Mater. Chem. Phys. 291 (2022) 126682
[18] H.H. Mohammed, R.A. Anaee, R.S. Noor, A.W. Muthana, Int. J. Electrochem. Sci. 8 (2013) 12402
[19] A. Merzah, H. Atwan, R. Anaee, J. Mech. Eng. Res. Dev. 44 (2021) 9
[20] M. Liu, Y.H. Wu, S.X. Luo, C. Sun, Werkstofftech. 41 (2010) 228
[21] H. Abdullah, R. Anaee, A. Khadom, A. Talib, A. Malik, M. Kadhim, Results Chem. 6 (2023) 101035
[22] A. Al-Ghaban, H. Abdullah, R. Anaee, Sh. Naser, A. Khadom, J. Eng. Res. 12 (2024) 299
[23] A. M. Ahmed Alwaise, Raqeeb H. Rajab, Adel A. Mahmood, Mohammed A. Alreshedi, Exp. Theo. NANOTECHNOLOGY 8 (2024) 67
[24] R.A. Jessam, S.S.H., AIP Conf. Proc. 3002 (2024) 040003
[25] H.A. Abdulaah, A.M. Al-Ghaban, R.A. Anaee, A.A. Khadom, M.M. Kadhim, J. Electrochem. Sci. Eng. 13 (2023) 115
[26] R. Anaee, H. Abdullah, Sh. Jawad, M. Jabar, Iraqi J. Mech. Mater. Eng. 17 (2017) 159
[27] N. M. Slaber, J. S. Kith, Exp. Theo. NANOTECHNOLOGY 9 (2025) 9
[28] H. Firouzi-Nerbin, F. Nasirpouri, E. Moslehifard, J. Alloys Compd. 822 (2020) 153712
[29] H. Mezher Jedy, R.A. Anaee, A.A. Abdullah, T. Mathew, J. Bio Tribo Corros. 7 (2021) 599
[30] H. Mezher Jedy, R.A. Anaee, A.A. Abdullah, Eng. Technol. J. 39 (2021) 565
[31] T. Abd Alkarim, K. Al Azawi, R. Anaee, Biochem. Cell. Arch. 21 (2021) 3557
[32] Sh. Naser, R. Anaee, H. Jaber, A. Khadom, Inorg. Chem. Commun. 165 (2024) 112478
[33] Sh. Naser, R. Anaee, H. Jaber, Adv. Mater. Process. Technol. 23 (2024) 59
[34] Sh. Naser, R. Anaee, H. Jaber, Chem. Afr. 58 (2023) 55
[35] Z.S. Aziz, R.A. Anaee, M.H. Abd, S.A. Naser, AIP Conf. Proc. 2475 (2023) 040016
[36] N.J. Al-Bahnam, Pramana 92 (2019) 27
[37] N. Hikmat, A. Farhan, R. Anaee, J. Al-Nahrain Univ. 12 (2009) 23
[38] R. Anaee, Arab J. Sci. Eng. 39 (2014) 153
[39] S. Abdul Maged, R. Anaee, M. Mathew, Int. J. Corros. Scale Inhib. 12 (2023) 275
[40] N.J. Al-Bahnam, K.A. Ahmad, A.I. Aboo Al-Numan, Phys. Lett. A 381 (2017) 616
[41] R. Anaee, Asian J. Chem. 26 (2014) 4469
[42] H. Abdullah, R. Anaee, A. Khadom, Int. J. Corros. Scale Inhib. 11 (2022) 1355
[43] N.J. Al-Bahnam, K.A. Ahmad, A.A. Rasheed, Int. J. Nanoelectron. Mater. 9 (2016) 165

Exp. Theo. NANOTECHNOLOGY 9 (2025) 449-463